Journal of Communications Technology and Electronics, Vol. 49, No. 7, 2004, pp. 806–815. Translated from Radiotekhnika i Elektronika, Vol. 49, No. 7, 2004, pp. 859–868.

MICROWAVE ELECTRONICS

On Oscillation Synchronization in a Distributed Active System Containing an Electron Beam Interacting with a Backward Electromagnetic Wave

A. E. Khramov

Received August 28, 2002

Abstract—A distributed active system in which an electron beam interacts with a backward electromagnetic wave is considered. Oscillation synchronization and the characteristics of spatial–temporal oscillations in this system are investigated. Physical processes developing during transition of the system to the synchronization mode are studied.

INTRODUCTION

Synchronization of various self-oscillatory systems by an external control signal has recently aroused considerable interest, which is indicated by a lot of publications in the field (see, e.g., [1–5] and the references cited therein). However, the effect of the external signal on processes in self-oscillators has been thoroughly studied only in the case of systems with pronounced resonance properties, especially Thompson systems. These self-oscillators are systems with a finite number of degrees of freedom and can be reduced to finite-dimensional models (described by systems of ordinary differential equations or mappings). Huygens discovered the synchronization effect in such systems as early as the 17th century [6]. Fundamental investigations of synchronization of finite-dimensional systems were described in classic studies by Andronov, Vitt, Teodorchik, Van der Pol, Khokhlov, and many other authors. External signal synchronization and mutual synchronization of reflex klystrons (which are resonant microwave electronic self-oscillators) were thoroughly investigated in [7, 8]. Synchronization of chaotic oscillations in nonlinear finite-dimensional dynamic systems exhibiting dynamic chaos has been of particular interest in the last few decades [3, 5, 9, 10].

Nonautonomous oscillations of distributed self-oscillatory systems have not been so comprehensively studied. An example of a classical distributed self-oscillatory microwave electronic system is a backward-wave tube (BWT), where microwave radiation is produced as a result of interaction between an electron beam and a backward electromagnetic wave synchronous with the beam. The effect of an external harmonic signal on the BWT oscillation has been investigated theoretically and experimentally [11–16]. In [11], an external signal introduced into a sectional slow-wave structure via a beam was considered. This approach, which was applied to analyze synchronization at a higher harmonic frequency, initiated the development of relativistic Doppler microwave frequency multipliers. The characteristics of BWT synchronous and asynchronous modes were obtained in [17, 18] within the framework of the stationary theory based on the synchronization equation proposed by Adler [19].

An active medium containing a helical electron beam that interacts with a counter-propagating electromagnetic wave (a counterpropagating-wave cyclotron-resonance maser (CRM)) was considered in [20–26], where certain aspects and peculiarities of synchronization of this medium by an external harmonic signal were investigated. Particular attention was given to the analysis of physical processes in a nonautonomous counterpropagating-wave CRM. Synchronization and concurrent oscillations of superpower microwave virtual-cathode oscillators were investigated experimentally and numerically in [27–29].

However, the studies mentioned above do not provide a comprehensive description of synchronization in distributed self-oscillatory systems based on interaction between an electron beam and the electromagnetic field, such as a system containing an electron beam interacting with a backward electromagnetic wave (below, this system is referred to as an EB–BEW system). Synchronization of this distributed self-oscillatory system can be thoroughly investigated using simulations based on the nonlinear nonstationary BWT theory.

In this paper, the elementary nonlinear nonstationary BWT theory involving the method of slowly varying amplitudes [30, 31] is applied to investigate the effect of an external harmonic signal on self-oscillations in an EB–WEW system. The analysis is performed using the simplest one-parameter model describing processes that develop when a rectilinear electron beam interacts with a backward wave in a transmission line [32, 33]. Therefore, it is interesting to

thoroughly study processes in a nonautonomous BWT based on the aforementioned simple theoretical model.

1. THE ORIGINAL EQUATIONS

The effect of an external harmonic signal on self-oscillations excited in an EB–BEW system is investigated using the standard equations of the nonstationary nonlinear BWT theory [30, 31, 34]

$$\frac{\partial^2\theta}{\partial\xi^2} = -A^2\mathrm{Re}\{F\exp(j\theta)\}, \quad (1)$$

$$\frac{\partial F}{\partial\tau} - \frac{\partial F}{\partial\xi} = -\frac{A}{\pi}\int_0^{2\pi}\exp(-j\theta)d\theta_0. \quad (2)$$

Equation (1) is the equation of electron motion in the presence of the synchronous electromagnetic wave field, and Eq. (2) is the equation describing excitation of a backward spatial harmonic of the electromagnetic wave. Here, θ is the electron phase in the presence of the wave field, $\xi = x/L$ is the longitudinal coordinate normalized to length of the interaction space L, $\tau = (t - xv_0)/(Lv_0 + Lv_g)$ is the dimensionless time, v_0 is the velocity of the electron flow entering the system, v_g is the group velocity of the electromagnetic wave at the synchronization frequency, F is the slowly varying complex amplitude of the wave field, $A = 2\pi CN$ is the dimensionless parameter corresponding to the dimensionless length of the interaction space (note that an increase in parameter A can be interpreted as an increase in the electron beam current), C is the Pierce amplification parameter [35], and N is the tube electrical length.

Equations (1) and (2) are combined with the following initial and boundary conditions:

$$F(\tau = 0, \xi) = f^0(\xi), \quad \theta(\xi = 0) = \theta_0,$$
$$\theta_0 \in [0, 2\pi], \quad \frac{\partial\theta}{\partial\xi}(\xi = 0) = 0. \quad (3)$$

An external harmonic control signal is applied to the collector end of the system, $\xi = A$ and described as $F(\xi = A) = F_0\exp(j\Omega\tau)$, where F_0 is the external signal amplitude and Ω is the difference between the frequencies of the external signal and cold synchronization ($\hat{\omega}$).

It has been shown [31–33, 36] that, in model (1)–(3), self-oscillations are self-excited at $A \approx 1.98$. When $A > 1.98$, the system exhibits one-frequency stationary oscillations. At $A \approx 2.9$, the output signal is self-modulated, so that two-frequency BWT oscillations are observed. At larger values of A, the oscillation spectrum becomes more intricate. When $A > 5.5$, the BWT exhibits chaotic oscillations.

2. ANALYSIS OF THE SYNCHRONOUS AND ASYNCHRONOUS MODES BASED ON THE STATIONARY THEORY

Following the approach developed in [17, 18], let us consider the bandwidth of phase synchronization and self-oscillation characteristics in the case in which the BWT stops operating in the synchronization mode. It is assumed that external signal E_0 applied to the BWT collector end has a low level and affects only the phase relationships for output signal E_{out}. Then, variations in the output signal amplitude are low: $\Delta E_{out} \ll E_{out}$. Therefore, one can neglect this variation compared to the value of E_{out}. Then, if the frequency of the external signal and BWT oscillation eigenfrequency are different, there is a phase difference, φ, between the output field oscillations in the autonomous and nonautonomous modes. This is due to a change in the conditions for the interaction between the traveling wave field and electron beam. Let us express the phase difference in terms of instant phase difference α between the field $E_{out} = E(0)$ of the nonautonomous BWT and control signal E_0 at the system output as

$$\varphi = -(|E_0(0)|/|E(0)|)\sin\alpha. \quad (4)$$

Expression (4) is valid both within and beyond the synchronization band. Instant phase difference α between the field (with frequency ω) of the system being synchronized and external signal can be represented as $\omega - \Omega = d\alpha/d\tau$. Introducing frequency ω_0 of autonomous oscillations, expression (4) can be modified to the form

$$\omega - \omega_0 = d\alpha/d\tau + \Omega - \omega_0. \quad (5)$$

In the synchronization mode, $\alpha = \mathrm{const}$ and $d\alpha/d\tau = 0$.

Let us find the variation of BWT output signal phase φ due to the variation of the BWT oscillation frequency caused by the external field. To obtain this, one should know field distribution $E(\xi)$ along the structure. This distribution can be determined using the method of successive approximations [17], according to which the first approximation of the field distribution along the interaction space is [35]

$$E(\xi) = E_0\exp j\beta_0(\xi - A)$$
$$\times[1 - A^3(\mathrm{Re}\Psi(\Phi_0) + j\mathrm{Im}\Psi(\Phi_0))], \quad (6)$$

where function $\Psi(\Phi_0)$ has the form typical of quadratic bunching [35]

$$\Psi(\Phi_0) = [2(\exp(-j\Phi_0) - 1)$$
$$+ j\Phi_0(\exp(-j\Phi_0) + 1)]/\Phi_0^3.$$

The quantity $\Phi_0 = (\beta_e - \beta_0)\xi$ is the relative angle of the electron transit through the interaction space, where $\beta_0 = \hat{\omega}/v_{ph}$ and $\beta_e = \hat{\omega}/v_0$.

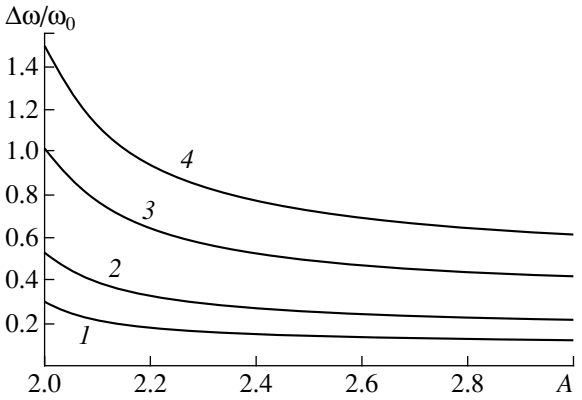

Fig. 1. Synchronization bandwidth $\Delta\omega/\omega_0$ vs. control parameter A obtained at E_0/E_{out} = (*1*) 0.1, (*2*) 0.15, (*3*) 0.3, and (*4*) 0.45.

Then, according to (6), the phase of the BWT output field respective to the control signal phase can be determined as

$$\psi = -\beta_0 A + \arctan\left(\frac{A^3 \mathrm{Im}\Psi(\Phi_0)}{1 + A^3 \mathrm{Re}\Psi(\Phi_0)}\right). \quad (7)$$

Let us find the variation of the field phase (and, hence, the variation of the oscillation frequency) caused by the external signal affecting the system. Developing phase ψ as a series in transit angle Φ_0 about the point corresponding to autonomous oscillation frequency ω_0 and assuming that the frequency variation is small,[1] we obtain

$$\psi = \psi_{\omega_0} + \left[\frac{\partial}{\partial\Phi_0}\arctan\left(\frac{A^3 \mathrm{Im}\Psi(\Phi_0)}{1 + A^3 \mathrm{Re}\Psi(\Phi_0)}\right)\right]_{\omega_0} \Delta\Phi_0, \quad (8)$$

where $|\Delta\Phi_0| \ll 1$. Let us pass from quantity $\Delta\Phi_0$ to the frequency variation. Differentiating function $\Phi_0(\omega)$ and taking into account the relationship between the wave group and phase velocities, the expression for the phase difference between the field of the synchronized BWT and control signal at the system output can be represented as [17]

$$\varphi = \frac{\omega_0 - \omega}{\omega_0}\frac{A}{C}\left(1 + \frac{v_{ph}}{v_g}\right) \times \left[\frac{\partial}{\partial\Phi_0}\arctan\left(\frac{A^3 \mathrm{Im}\Psi(\Phi_0)}{1 + A^3 \mathrm{Re}\Psi(\Phi_0)}\right)\right]_{\omega_0}. \quad (9)$$

[1] The latter means that field phase expansion (7) is truncated to the first term.

Relationships (4), (5), and (9) yield the differential equation for phase difference α between the nonautonomous BWT output field and external signal

$$d\alpha/d\tau + \omega_0\kappa\sin\alpha - (\Omega - \omega_0) = 0, \quad (10)$$

where coefficient κ has the form

$$\kappa = \frac{C}{A}\frac{E_0}{E_{out}} \times \left(1 + \frac{v_{ph}}{v_g}\right)^{-1} \Big/ \left[\frac{\partial}{\partial\Phi_0}\arctan\left(\frac{A^3 \mathrm{Im}\Psi(\Phi_0)}{1 + A^3 \mathrm{Re}\Psi(\Phi_0)}\right)\right]_{\omega_0}. \quad (11)$$

Equation (10) describes the behavior of the BWT output field phase in the case in which the BWT is affected by a microwave field. This equation was first obtained in [18]. The synchronization mode corresponds to a constant phase difference between the output and control signals, $d\alpha/d\tau = 0$. The maximum value of the frequency difference $(\omega_0 - \Omega_s)$ at which synchronization is observed is determined by the condition $\sin\alpha = \pm 1$ (Ω_s is the frequency corresponding to the boundary of the synchronization region). Then, according to Eq. (10), the synchronization bandwidth $\Delta\omega = 2|\omega_0 - \Omega_s|$ can be found from the relationship

$$\Delta\omega/\omega_0 = 2\kappa. \quad (12)$$

Relationships (11) and (12) imply that the synchronization bandwidth is mainly governed by control signal amplitude E_0 and structure length A. The quantity $\Delta\omega/\omega_0$ is proportional to the ratio of the amplitudes of the control and BWT output signals.

Synchronization bandwidth $\Delta\omega/\omega_0$ versus control parameter A is depicted in Fig. 1 at various values of E_0/E_{out}. One can see that, as system length A increases, synchronization bandwidth $\Delta\omega/\omega_0$ decreases. At large interaction space length A and various external signal amplitudes, the synchronization bandwidth can be approximated by a power function of the form $\Delta\omega/\omega_0 \sim 1/A$.

The analysis of Eq. (10) shows that, when $\kappa \geq |\omega_0 - \Omega|$, quantity α asymptotically approaches a constant value as $\tau \longrightarrow \infty$, which corresponds to self-oscillation synchronization in an active medium. On the contrary, when $\kappa < |\omega_0 - \Omega|$, there is no constant, i.e., time-independent, phase difference between the signal generated by a nonautonomous BWT and the control signal. The system exhibits beating with period α. Equation (10) implies that the self-modulation period tends to infinity as the boundary of the synchronization region is approached, T_a. As external signal amplitude $|\omega_0 - \Omega| \longrightarrow \kappa$ grows, the self-modulation period increases at equal frequency differences $|\omega_0 - \Omega|$. As the frequency

detuning increases, the self-modulation period decreases approaching a constant value at different external signal amplitudes. Simultaneously, the output signal modulation function approaches a sinusoid as the frequency difference $|\omega_0 - \Omega|$ increases.

Let us determine how Eq. (10), first obtained for a BWT [17, 18], can be applied to describe the spatial dynamics of a nonautonomous BWT. The determining characteristic of BWT nonautonomous oscillations is coefficient κ, expressed by (11). Taking into account relationships (6) and (7) for the amplitude distribution and field phase, this coefficient can be regarded as a function of longitudinal coordinate $\kappa = \kappa(\xi)$.

Let is consider phase difference α between nonautonomous BWT field $E(\xi)$ and external signal $E_0(\xi)$ as a function of the coordinate and time, $\alpha = \alpha(\tau, \xi)$. Taking into account that $\kappa = \kappa(\xi)$, we also consider a solution to Eq. (10) at any point of the interaction space. Definition (11) implies that function κ decreases as ξ increases and, at a large length of the interaction space, $\kappa(\xi) \sim 1/\xi$.

As was shown above, the synchronization mode is realized when $\kappa \geq |\omega_0 - \Omega|$. Then, at a small length of the interaction space and sufficiently small frequency detuning, the synchronization mode corresponding to a constant phase, $\alpha(\tau, \xi) = \text{const}$, is always observed. However, as the coordinate grows and, accordingly, quantity $\kappa(\xi)$ decreases, the latter may take a value less than $|\Omega - \omega_0|$ at a certain point of the interaction space $\xi = \xi^*$. Then, synchronization collapses.

This means that, in the interaction space of the tube operating in the asynchronous mode, we can find two characteristic regions: (i) the region of length A_s ($A_s = A - \xi^*$ is referred to as the synchronization length) where synchronization is observed and (ii) the region of the length $A - A_s$ where the synchronization mode collapses. Thus, in the asynchronous mode, the nonautonomous system exhibits oscillations the frequency and oscillation shape of which vary along the longitudinal coordinate of the interaction space. The characteristic frequency $\omega(\xi)/\omega_0$ of self-oscillations excited in the nonautonomous system in the asynchronous mode versus spatial coordinate ξ is shown in Fig. 2a at various frequency differences $|\Omega - \omega_0|/\kappa$. It is seen that synchronization length A_s, corresponding to $\omega(\xi)/\omega_0 = 1$, increases as the frequency difference decreases. When $\xi < A_s$, frequency $\omega(\xi)$ rapidly grows, after which it becomes virtually independent of the coordinate. Figure 2b shows synchronization length A_s versus frequency detuning $|\Omega - \omega_0|/\kappa$. Synchronization region boundary Ω_s (marked by an arrow in Fig. 2b), corresponds to the case in which the synchronization length is equal to the system length, $A_s \equiv A$.

Thus, analysis of the BWT synchronous and asynchronous nonautonomous modes based on synchronization equation (10) shows that the synchronization bandwidth is determined by the external field amplitude and, substantially, depends on BWT dimensionless length A (electron beam current). In the BWT asynchronous mode, the interaction space is divided into two characteristic regions: the region of microwave field oscillations synchronous with the external signal and the region of asynchronous dynamics. As the synchronization region boundary is approached, synchronization region length A_s tends to BWT length A. In the synchronization mode, oscillations at the external signal frequency are observed within the entire interaction space.

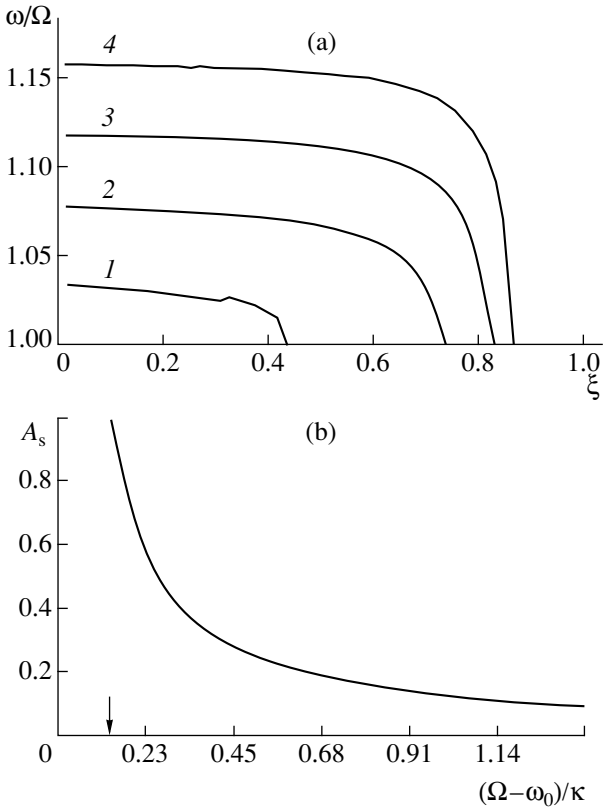

Fig. 2. (a) Oscillation frequency vs. interaction space coordinate ξ obtained at various detuning values: $|\Omega - \omega_0|/\kappa =$ (*1*) 0.23, (*2*) 0.45, (*3*) 0.68, and (*4*) 0.91. (b) Synchronization length A_s vs. $|\Omega - \omega_0|/\kappa$.

3. NONLINEAR NONSTATIONARY ANALYSIS OF SYNCHRONIZATION

Numerical integration of BWT nonlinear nonstationary equations (1)–(3) was applied to study BWT self-oscillation synchronization. The solution of system of equations (1)–(3) involved a difference scheme of second-order accuracy similar to that described in [34]. The time and coordinate steps were chosen to be $\Delta\tau = 0.004$ and $\Delta\xi = 0.008$, respectively.

The map of the system oscillation modes represented in the plane of control parameters—frequency Ω/ω_0 and external signal amplitude F_0—is displayed in

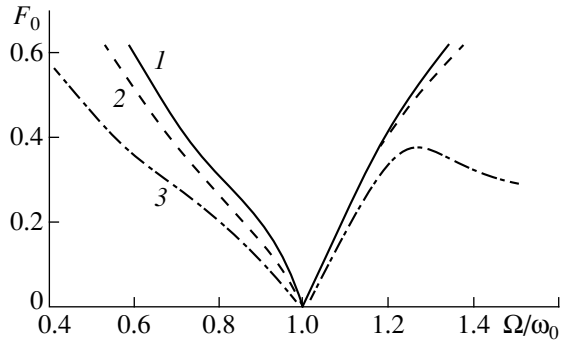

Fig. 3. The plane of control parameters—external signal frequency Ω and amplitude F_0—divided into regions corresponding to characteristic nonautonomous oscillation modes realized in a BWT: (*1*) synchronization mode, (*2*) quasi-synchronization region, and (*3*) change in the character of self-modulation.

Fig. 3 in the case in which the system length is $A = 2.2$. The regions of the characteristic dynamic modes exhibited by the nonautonomous system under study are marked on this map. When the frequencies of the external signal (Ω) and autonomous system oscillation (ω_0) have close values, the BWT exhibits the synchronization mode. Output signal frequency ω is governed by the external signal frequency, and output signal amplitude $|F(\xi = 0, \tau)|$ becomes constant after the transient process finishes (stationary oscillation). When the values of control parameters correspond to an intersection of the synchronization region boundary, the system passes to the mode of output signal modulation. Then, signal amplitude $|F(\xi = 0, \tau)|$ starts to vary periodically in time.

Investigation of base frequency ω of the output field $F = |F(\tau)|\exp(j\omega\tau)$ as a function of the external control signal parameters has shown that the region of frequency ω locking is substantially wider than the region of stationary oscillation, the latter being marked on the mode map as the synchronization region. When the external signal frequency exceeds the autonomous oscillation frequency ($\Omega/\omega_0 > 1.0$) and external signal amplitude F_0 is small, the frequency-locking region coincides with the boundary of the self-modulation region (and, accordingly, the synchronization region). Note that, when $\Omega/\omega_0 < 1.0$, curve *2* and the boundary of the synchronization region do not coincide at any indefinitely small amplitude F_0 of the external signal.

The nonautonomous system oscillation mode corresponding to locking of high-frequency (HF) oscillation frequency ω is referred to as the quasi-synchronization mode. In this mode, HF radiation is generated at the frequency $\omega \approx \Omega$, and output field amplitude $|F|$ may slowly vary at a characteristic time scale. When the system leaves the quasi-synchronization region, the oscillation base frequency approaches the autonomous oscillation frequency as the detuning of external signal frequency Ω from quasi-synchronization region boundary Ω_s increases.

Figures 4 and 5 show the quasi-synchronization bandwidth versus external signal amplitude F_0 at various BWT lengths (Fig. 4) and versus system dimensionless length A at various external signal amplitudes F_0 (Fig. 5). Let us analyze these dependences in detail.

It follows from the results presented in Fig. 4 that, at small system lengths, the quasi-synchronization bandwidth (solid line) increases with external signal amplitude as a virtually linear function. This confirms the results obtained in the previous section: at small external field amplitudes, the synchronization bandwidth linearly grows with E_0 (see relationships (11) and (12)).

The dependence of the synchronization bandwidth (Fig. 4, dashed line) on external signal amplitude F_0 deviates from a linear function. When BWT dimensionless length A is small, the quasi-synchronization bandwidth substantially exceeds the synchronization band-

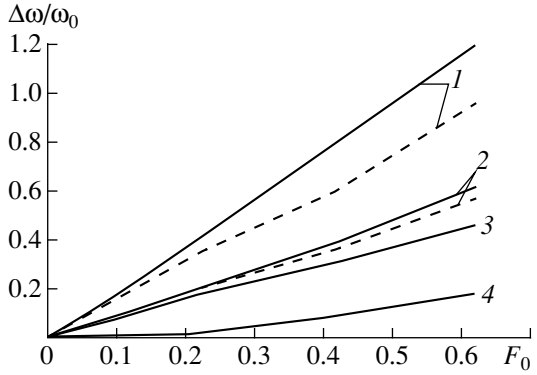

Fig. 4. Synchronization (dashed line) and quasi-synchronization (solid line) bandwidths vs. external signal amplitude F_0/F_{out} at $A = (1)$ 2.1, (*2*) 2.4, (*3*) 2.8, and (*4*) 3.5 (F_{out} is the output signal amplitude in the autonomous mode).

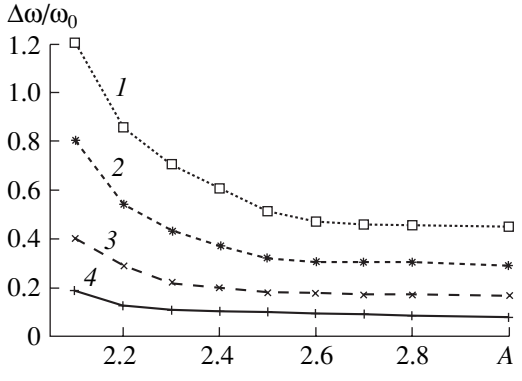

Fig. 5. Synchronization bandwidth $\Delta\omega/\omega_0$ vs. system length A obtained at various control signal amplitudes F_0/F_{out} (calculations are performed using nonlinear nonstationary model (1)–(3)): $F_0/F_{out} = (1)$ 0.45, (*2*) 0.3, (*3*) 0.15, and (*4*) 0.1.

width. As A grows, the difference between the synchronization and quasi-synchronization bandwidths decreases. As the system length approaches the value $A = 2.9$, at which the autonomous system exhibits self-modulation of the output signal, the synchronization region, where stationary oscillations are generated at the external signal frequency, disappears. At the same time, the nonautonomous system retains the quasi-synchronization mode with output signal frequency $\omega = \Omega$ and time-dependent output signal amplitude $|F|$ (see Fig. 4, curves *3* and *4*).

Synchronization bandwidth $\Delta\omega/\omega_0$ versus parameter A is shown in Fig. 5. Comparing the simulation results presented in Fig. 5 and the results obtained via stationary analysis of BWT synchronization (see Fig. 2a), one can draw the conclusion that, at a small system length and small external signal amplitude, the stationary analysis of synchronization is in good agreement with the solution of the complete system of nonstationary BWT equations. As parameter A grows, the synchronization bandwidth $\Delta\omega/\omega_0$ decreases. As a function of F_0, the synchronization bandwidth becomes virtually independent of A when $A > 2.2$–2.6.

Curve *3* on the mode map (Fig. 3) corresponds to a change in the character of self-modulation. When the synchronization region boundary is crossed (curve *1*), self-modulation of output signal amplitude $|F(\tau)|$ is observed. The self-modulation function is rather intricate and far from harmonic. When input signal amplitude F_0 is small, the self-modulation amplitude is excited in the hard mode, i.e., the amplitude of output signal modulation oscillations is finite on the boundary of the synchronization characteristic beak. When the control signal level is large, the self-modulation amplitude is softly excited and rapidly reaches its maximum. As detuning from the boundary of the synchronization characteristic beak grows, the self-modulation amplitude slowly decreases. When curve *3* is crossed, the self-modulation function approaches a sinusoid, which simplifies the spectrum of the output signal of the nonautonomous BWT operating in the asynchronous mode. When the boundary of the synchronization characteristic beak is crossed, the self-modulation frequency is excited in the soft (hard) mode at small (large) values of F_0.

All the results obtained in this section within the framework of the one-wave nonlinear nonstationary theory based on relationships (1)–(3) are valid only at small external field amplitudes at the collector end of the system and small frequency detuning of the external harmonic signal respective to autonomous oscillation (precisely the case considered in the paper). Otherwise, the nonautonomous dynamics of the system being studied should be analyzed using more complicated models, such as ones based on direct integration of the Maxwell–Vlasov equations using the particle method (see, e.g., [37, 38]).

4. PHYSICAL PROCESSES IN A NONAUTONOMOUS BACKWARD-WAVE OSCILLATOR

Consider physical processes observed during transformation of oscillation modes in a nonautonomous active EB–BEW system.

Let us investigate the processes in the system that develop when the device oscillation frequency is locked by an external signal with amplitude F_0 and frequency Ω. The HF oscillation frequency is determined as correction ω_0 to cold synchronization frequency $\hat{\omega}$. Frequency ω_0 depends on phase $\varphi_F(\xi, \tau)$ of field $F(\xi, \tau) = |F(\xi, \tau)|\exp\{j\varphi_F(\xi, \tau)\}$. In the case of one-frequency HF oscillation, the frequency correction can be represented in the form

$$\omega_0 = \lim_{T \to \infty} \varphi_F(0, \tau)/\tau. \quad (13)$$

If it is assumed that phase $\varphi_F(\xi, \tau)$ is a periodic function with a period of 2π, i.e., if the function

$$\bar{\varphi}_F(\xi, \tau) = \varphi_F(\xi, \tau) \bmod 2\pi, \quad (14)$$

is considered, $\bar{\varphi}_F$ exhibits periodic behavior with the period $1/\omega_0$ (Fig. 6a, $A = 2.2$).

In nonautonomous oscillation modes, frequency ω_0, which is determined by relationship (13), characterizes the temporal scale of BWT HF oscillation.

Oscillation quasi-synchronization, i.e., generation of HF radiation at the frequency $\omega_0 = \Omega$, corresponds to oscillations of phase $\bar{\varphi}_F$ at frequency Ω. As was shown above, output field amplitude $|F|$ may exhibit periodic self-modulation.

Consider the behavior of the amplitude and phase of field $F(\xi, \tau)$ in a BWT operating in the nonautonomous mode. The spatial-temporal distributions of the amplitude and phase of field F calculated at equal values of amplitude F_0 and various external signal frequencies are displayed in Figs. 6b–6d.

The results presented in Fig. 6 confirm the analysis of the spatial–temporal dynamics exhibited by a nonautonomous active EB–BEW medium (see Section 2). One can see in Fig. 6b that, in the asynchronous mode (which differs from the quasi-synchronization mode), the interaction space can be formally divided into two regions. In one region, which is adjacent to system collector end $\xi = A$, phase $\bar{\varphi}_F$ oscillates at external signal frequency Ω. In a rather narrow region of the interaction space, field phase $\bar{\varphi}_F$ varies stepwise by π. In the region near the system output $\xi = 0$, the phase oscillates at frequency ω, which is different from Ω. Oscillation frequency ω approaches autonomous oscillation frequency ω_0 as detuning of external signal frequency Ω

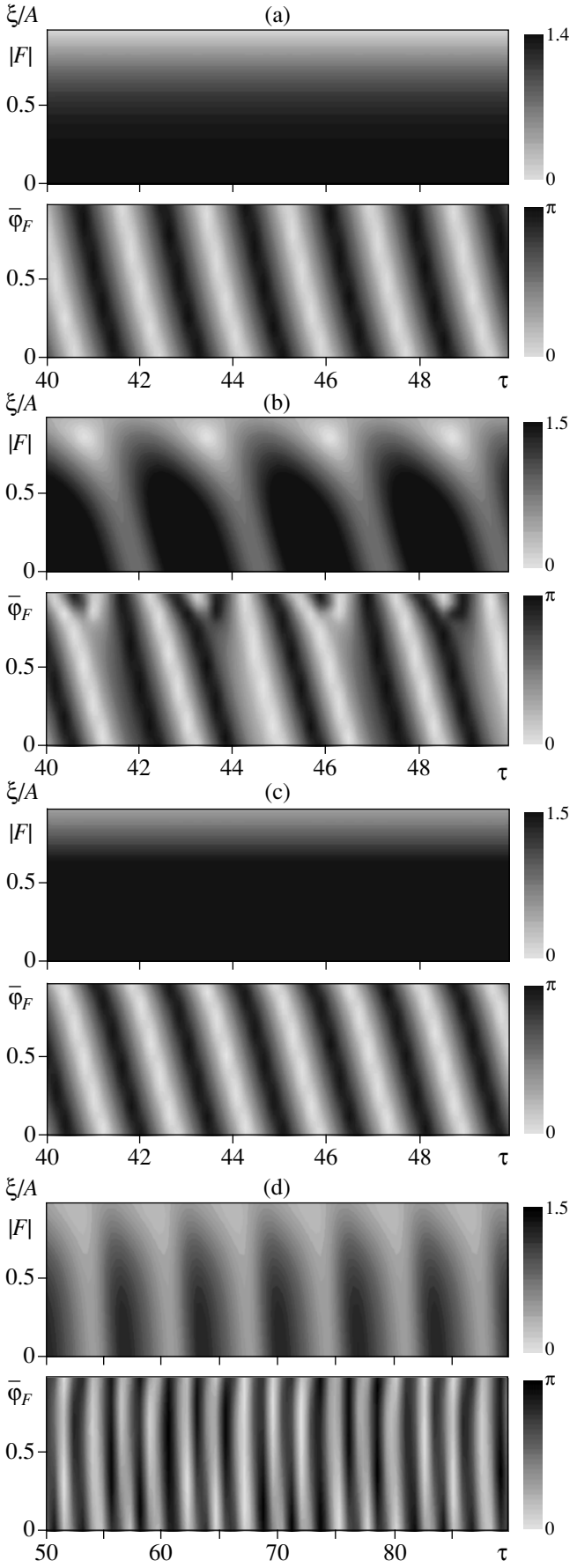

from the quasi-synchronization region boundary grows.

Thus, in the nonautonomous BWT interaction space, two characteristic regions of spatial–temporal oscillations are formed: the region where temporal oscillations are synchronized with the control signal and the region where the frequency of oscillations differs from that of the control signal. These two regions are separated by a narrow region where field phase $\bar{\varphi}_F$ exhibits stepwise variations.

In the synchronization and quasi-synchronization regions, oscillations at external signal frequency Ω are observed over the entire interaction space. In the projection of distribution $\bar{\varphi}_F(\xi, \tau)$ (Figs. 6c and 6d), one can see a pattern identical to that obtained in the case of autonomous oscillations (see Fig. 6a), the latter being realized at the frequency $\omega_0 = \Omega$.

Note that the analytical theory of BWT phase synchronization based on the stationary linear theory does not describe the effect of synchronization characteristic beak splitting into the region of stationary oscillation at the external signal frequency and the region of self-modulation with base frequency locking by the external signal (quasi-synchronization). At the same time, this theory correctly predicts the appearance of two regions with different dynamics temporal scales in the asynchronous mode.

Let us introduce at each point in the interaction space frequency $\omega(\xi)$ determined according to formula (13), in which the field phase at the system output $\xi = 0$ is replaced by quantity $\varphi_F(\xi)$ at arbitrary point ξ of the interaction space. Calculated dependence $\omega = \omega(\xi)$ is depicted in Fig. 7a.

In the quasi-synchronization mode, the oscillation frequency satisfies the equality $\omega(\xi) = \Omega$ in the entire interaction space (output signal amplitude $|F|$ slowly varies in time as compared to frequency Ω).

In modes different from the quasi-synchronization mode, the spatial-temporal dynamics in the interaction space become more complicated. In the region adjacent to the system collector end $\xi = A$, oscillations at the external signal frequency are observed. In the region located at a larger distance from the collector end,

Fig. 6. Surfaces of spatial–temporal distributions of field amplitude $|F|$ and phase φ_F projected onto the (τ, ξ) plane in the cases of BWT (a) one-frequency autonomous and (b–d) nonautonomous oscillation modes. The results are obtained at the same amplitude $F_0/F_{out} = 0.3$ and various external signal frequencies Ω: (b) $\Omega/\omega_0 = 1.71$ (the periodic self-modulation mode different from the quasi-synchronization mode), (c) $\Omega/\omega_0 = 1.17$ (the stationary oscillation mode, the synchronization region), and (d) $\Omega/\omega_0 = 0.70$ (the quasi-synchronization mode, the output signal is modulated).

the nonautonomous oscillation frequency is rapidly detuned from external field frequency Ω. As detuning $|\Omega - \omega_0|$ grows, synchronization length A_s decreases.

The dependence of synchronization length A_s on the frequency detuning of the distributed self-oscillatory system oscillations and external signal is depicted in Fig. 7b. Comparing these results with those presented in Fig. 2b, which shows the theoretical dependence of A_s on the frequency detuning, one can conclude that simulation confirms the dependence predicted by the stationary analysis well. As $\Omega \longrightarrow \Omega_s$ (Ω_s is the frequency corresponding to the synchronization characteristic beak), synchronization length A_s tends to the total length of the interaction space. When the detuning $|\Omega - \omega_0|$ is large, the synchronization length is small and independent of detuning variations.

Comparing dependences $\omega(\xi)$ obtained using simulation of nonstationary system (1)–(3) (Fig. 7a) with those predicted by the stationary linear theory (see Fig. 2a), one can conclude that, though the oscillation frequency exhibits a qualitatively similar behavior, the dependences have different forms. The main difference is that the oscillation frequency rapidly changes at coordinate $\xi = A - A_s$. At large detuning values, the frequency is stabilized and does not vary over the interaction space. When the external signal frequency is slightly detuned from the synchronization characteristic beak, the frequency exhibits several rapid variations over the interaction space length.

This difference between the results provided by simulations and the analytical theory can be attributed to fundamentally nonlinear effects that occur during interaction between the electron beam and backward wave and are not taken into account by the linear theory. The regions of the interaction space where nonautonomous self-oscillation frequency ω exhibits rapid variations are determined by electron rebunching in the beam. This corresponds to the fact that the amplitude of the first harmonic of the bunched beam current

$$I(\xi) = \frac{1}{\pi}\int_0^{2\pi} \exp(-j\theta)d\theta_0$$

reaches its maximum within the length $\xi = A - A_s$ and decreases along interval A_s towards the BWT input $\xi = A$, where the external signal is applied. Simultaneously, the interior structure of the electron beam in the nonautonomous system is transformed. Thus, beam rebunching results in jumps of the phase of current $I(\xi)$ and $F(\xi)$ in the region $\xi \sim A - A_s$. As a result, when the synchronization region is left, the external signal effect manifests itself in violation of the phase relationships between the field and the current complex amplitudes

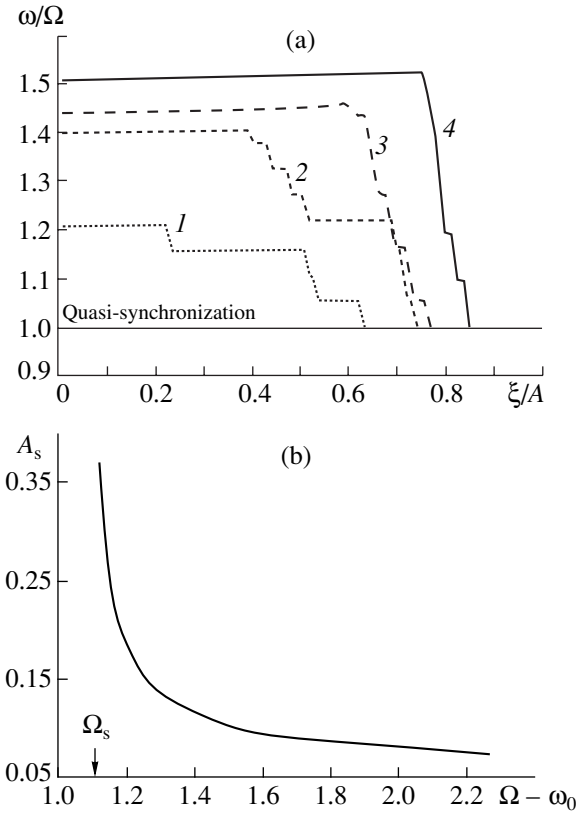

Fig. 7. (a) The characteristic self-oscillation frequency in various sections of the interaction space obtained at different external signal frequencies, $\Omega - \omega_0 = (1)$ 1.13, (2) 1.15, (3) 1.18, and (4) 1.28, and (b) synchronization length A_s vs. detuning ($A = 2.2$ and $F_0/F_{out} = 0.3$).

(F and I) that are valid in the stationary oscillation mode.

An additional distributed feedback is formed in the system as follows. The electron beam bunched in a strong field arrives at the system collector end $\xi = A$ at the velocity $v \approx v_0$ in the rebunched state. The field excited by the bunched beam current shifts at velocity v_g towards the system input end $\xi = 0$. The beam, which has been bunched in a weak field, induces now a strong field; and, in the presence of the latter, the electron beam is rebunched. The process is repeated with the period

$$T_A \sim 2(A - A_s)(1/v_0 + 1/v_g).$$

Thus, the output signal modulation modes observed when the synchronization region is left are determined by nonlinearity in the electron beam, which is caused by inertia of electrons and results in beam electron rebunching. A variation in the self-modulation period due to frequency detuning of the external signal from synchronization characteristic beak Ω_s is determined by a variation in synchronization length A_s and increases with growth of

frequency detuning $|\Omega - \omega_0|$. The latter is verified by calculations: self-modulation period T_A increases when external signal frequency Ω is detuned from autonomous oscillation frequency ω_0.

CONCLUSIONS

The effect of an external harmonic signal on self-oscillations in a BWT has been investigated. The characteristics of the synchronous mode have been considered, and it has been shown that a nonautonomous system exhibits both synchronization and quasi-synchronization modes. The former corresponds to stationary oscillation at the external signal frequency and the latter to oscillation at the base frequency determined by the control signal and slow variations of the output signal amplitude. Quasi-synchronization modes are associated with spatial–temporal oscillations excited over the entire interaction space at the external signal frequency. When the quasi-synchronization region is exited, two characteristic regions are formed in the interaction space. In one region (which has length A_s, referred to as the synchronization length), oscillations at the external signal frequency are observed. In the other region (of the length $A - A_s$), synchronization collapses and oscillations at a frequency different from that of the control signal are realized in the interaction space.

Note that it is important to study BWT nonautonomous modes taking into account relativistic effects, which is a topical problem in modern relativistic electronics. The reason is that these studies may facilitate investigations oriented to developing various modifications of microwave backward-wave oscillators.

ACKNOWLEDGMENTS

The author is grateful to D.I. Trubetskov for his interest in this work, fruitful discussions, and useful remarks. This work was supported by the Russian Foundation for Basic Research (project no. 02-02-16351), the scientific program "Universities of Russia–Fundamental Investigations," the Dinastiya Foundation, and the International Center of Fundamental Physics (Moscow).

REFERENCES

1. A. Pikovsky, M. Rosenblum, and J. Kurths, *Synchronization. A Universal Concept in Nonlinear Sciences* (Cambridge University Press, Cambridge, 2001).
2. V. S. Afraimovich, V. I. Nekorkin, G. V. Osipov, and V. D. Shalfeev, *Stability, Structures, and Chaos in Nonlinear Synchronization Networks*, Ed. by A. V. Gaponov-Grekhov and M. I. Rabinovich (IPF AN SSSR, Gorki, 1989) [in Russian].
3. N. F. Rulkov, M. M. Sushchik, L. S. Tsimring, and H. D. I. Abarbanel, Phys. Rev. E: Stat. Phys., Plasmas, Fluids, Relat. Interdiscip. Top. **51**, 980 (1995).
4. M. G. Rosenblum, A. S. Pikovsky, and J. Kurths, Phys. Rev. Lett. **76**, 1804 (1996).
5. L. M. Pecora, T. L. Carroll, G. A. Jonson, and D. J. Mar, Chaos **7**, 520 (1997).
6. C. Hugenii, *Horoloqium Oscillatorium* (Apud F. Muquet, Parisiis, France, 1673).
7. R. V. Khokhlov, Radiotekh. Elektron. (Moscow) **1**, 88 (1956).
8. V. B. Braginskii, S. D. Gvozdover, A. S. Gorshkov, and I. T. Trofimenko, Radiotekh. Elektron. (Moscow) **2**, 1048 (1957).
9. A. S. Dmitriev and V. Ya. Kislov, *Stochastic Oscillations in Radiophysics and Electronics* (Nauka, Moscow, 1989) [in Russian].
10. V. S. Anishchenko and T. E. Vadivasova, Radiotekh. Elektron. (Moscow) **47**, 133 (2002) [J. Commun. Technol. Electron **47**, 117 (2002)].
11. V. I. Kanavets, Vestn. Mosk. Univ., Ser. 3: Fiz., Astron., No. 2, 32 (1961).
12. M. J. Wong, G. D. Sims, and I. M. Stephenson, J. Electron. Control **11**, 684 (1961).
13. A. M. Kats, Elektron. Tekhnika. Ser. Elektronika SVCh, No. 5, 37 (1966).
14. G. P. Rapoport, Radiotekh. Elektron. (Moscow) **9**, 118 (1964).
15. G. P. Rapoport and A. A. Klushin, Radiotekh. Elektron. (Moscow) **9**, 1520 (1964).
16. V. A. Solntsev, Elektron. Tekhnika. Ser. Elektronika SVCh, No. 9, 30 (1966).
17. B. E. Zhelezovskii and E. V. Kal'yanov, *Microwave Device Multifrequency Modes* (Svyaz', Moscow, 1978) [in Russian].
18. B. E. Zhelezovskii and E. V., Kal'yanov, Vopr. Radioelektron. Ser. Elektron., No. 4, 44 (1965).
19. R. Adler, Proc. IRE **34**, 351 (1946).
20. D. I. Trubetskov and A. E. Khramov, Pis'ma Zh. Tekh. Fiz. **28** (18), 34 (2002) [Tech. Phys. Lett. **28**, 767 (2002)].
21. A. A. Koronovskii, D. I. Trubetskov, and A. E. Khramov, Izv. Vyssh. Uchebn. Zaved. Prikl. Nelin. Din. **10** (4), 47 (2002).
22. D. I. Trubetskov and A. E. Khramov, Izv. Akad. Nauk. Ser. Fiz. **66**, 1761 (2002).
23. A. A. Koronovskii, I. S. Rempen, D. I. Trubetskov, and A. E. Khramov, Izv. Akad. Nauk. Ser. Fiz. **66**, 1754 (2002).
24. A. A. Koronovskii, D. I. Trubetskov, and A. E. Khramov, Izv. Vyssh. Uchebn. Zaved. Radiofiz. **45**, 578 (2002).
25. D. I. Trubetskov and A. E. Khramov, Radiotekh. Elektron. (Moscow) **48**, 116 (2003) [J. Commun. Technol. Electron. **48**, 105 (2003].
26. A. E. Khramov, Izv. Akad. Nauk. Ser. Fiz. **67**, 1674 (2003).

27. V. P. Grigor'ev, A. G. Zherlitsyn, T. V. Koval', *et al.*, Pis'ma Zh. Tekh. Fiz. **14**, 2164 (1988).

28. W. Woo, J. Benford, D. Fittingoff, *et al.*, J. Appl. Phys. **65**, 861 (1989).

29. A. E. Khramov, Radiotekh. Elektron. (Moscow) **44**, 211 (1999) [J. Commun. Technol. Electron. **44**, 211 (1999)].

30. S. P. Kuznetsov and D. I. Trubetskov, *Electronics of Backward-Wave Tubes* (Sarat. Gos. Univ., Saratov, 1975), p. 135 [in Russian].

31. D. I. Trubetskov and A. P. Chetverikov, Izv. Vyssh. Uchebn. Zaved. Prikl. Nelin. Din. **2** (5), 3 (1994).

32. N. M. Ryskin, V. N. Titov, and D. I. Trubetskov, Dokl. Akad. Nauk **358**, 620 (1998) [Dokl. Phys. **43**, 90 (1998)].

33. N. M. Ryskin and V. N. Titov, Izv. Vyssh. Uchebn. Zaved. Prikl. Nelin. Din. **6** (1), 75 (1998).

34. N. S. Ginzburg, S. P. Kuznetsov, and T. N. Fedoseeva, Izv. Vyssh. Uchebn. Zaved. Radiofiz. **21**, 1037 (1978).

35. V. N. Shevchik and D. I. Trubetskov, *Analytical Calculation Methods in Microwave Electronics* (Sov. Radio, Moscow, 1970) [in Russian].

36. B. P. Bezruchko, S. P. Kuznetsov, and D. I. Trubetskov, *Nonlinear Waves. Stochasticity and Turbulence* (IPF AN SSSR, Gor'ki, 1980), p. 29.

37. I. V. Pegel', Izv. Vyssh. Uchebn. Zaved. Fiz. **34** (12), 62 (1996).

38. T. M. Anderson, A. A. Mondelli, B. Levush, *et al.*, Proc. IEEE **87**, 804 (1999).